The effect of oxidation on the electronic structure of the green fluorescent protein chromophore

E. Epifanovsky,[1,a)] I. Polyakov,[2] B. Grigorenko,[2] A. Nemukhin,[2,b)] and A. I. Krylov[1,c)]
[1]*Department of Chemistry, University of Southern California, Los Angeles, California 90089, USA*
[2]*Department of Chemistry, M.V. Lomonosov Moscow State University, Moscow 119991, Russia*

(Received 23 December 2009; accepted 7 February 2010; published online 18 March 2010)

Electronic structure calculations of the singly and doubly ionized states of deprotonated 4′-hydroxybenzylidene-2,3-dimethylimidazolinone (HBDI anion) are presented. One-electron oxidation produces a doublet radical that has blueshifted absorption, whereas the detachment of two electrons yields a closed-shell cation with strongly redshifted (by about 0.6 eV) absorption relative to the HBDI anion. The results suggest that the doubly oxidized species may be responsible for oxidative redding of green fluorescent protein. The proposed mechanism involves two-step oxidation via electronically excited states and is consistent with the available experimental information [A. M. Bogdanov, A. S. Mishin, I. V. Yampolsky, *et al.*, Nat. Chem. Biol. **5**, 459 (2009)]. The spectroscopic signatures of the ionization-induced structural changes in the chromophore are also discussed. © *2010 American Institute of Physics*. [doi:10.1063/1.3336425]

I. INTRODUCTION

The unique properties of green fluorescent protein (GFP) exploited in novel bioimaging techniques revolutionized many areas in life sciences.[1–3] The photophysics of GFP and other wild-type and mutated photoactive proteins have been a subject of many experimental and theoretical studies.[4,5] Yet, intrinsic electronic properties of the chromophores and their interactions with the protein matrix are not fully understood.

The absorption spectrum of the wild-type GFP has two broad bands at 3.13 eV (396 nm) and 2.60 eV (476 nm) assigned to the neutral and the anionic (deprotonated) forms of the chromophore, respectively. The fluorescence spectrum is also broad and has a maximum at 2.44 eV (508 nm). Detailed mechanistic studies demonstrated that while both the neutral and the anionic forms of the GFP chromophore are responsible for absorption, fluorescence occurs from the anionic form (see, for example, recent reviews[4,5] on the photophysics of GFP and references therein).

The absorption and fluorescence wavelengths and quantum yields can be controlled by structural modifications, and a number of GFP mutants and other photoactive proteins have been characterized.[5,6] The changes in photophysics can be due to structural modifications of the chromophore itself or in the surrounding protein. Moreover, the photochemical properties of some chromophores from the GFP family can be affected by light giving rise to so-called optical highlighting techniques. By using light of varying intensity and duration, the fluorescence can be turned on and off (photoswitching), and its spectrum (both wavelength and intensities) can be changed (photoconversion). Both reversible and irreversible photoconversion have been described in the literature.[5,7]

Photoconversion phenomena are not yet well understood at the molecular level. The established mechanisms involve photoinduced isomerizations (e.g., *cis-trans* transformation), changes in protein microenvironment, as well as more significant structural changes such as bond breaking, proton and charge transfer between the protein and the chromophore.[5,7] For example, the intensity of GFP fluorescence is increased by two orders of magnitude upon irreversible photoconversion by UV or visible light (4.9–2.6 eV) to the anionic form accompanied by the decarboxylation of an adjacent glutamine residue.[8,9] That also leads to a change in the absorption spectrum: increased absorbance of blue light and diminished absorbance in the UV region. In another FP, Dronpa, photoconversion between a protonated dark and an anionic bright forms is reversible and involves *cis-trans* isomerization.[10] A different photoconversion type is exemplified by Kaede FP, which can be irreversibly switched from green to red fluorescent form by the cleavage of a peptide bond leading to the extension of the π-system of the chromophore.[7]

Photoinduced redding of GFP is a photoconversion that has not yet been explained. It was observed[11] that under anaerobic conditions illumination of a GFP mutant (GFP-mut2) with blue light (2.5–2.7 eV or 460–500 nm) for several seconds results in red fluorescence at 1.8–2.0 eV (610–680 nm). Similar behavior was observed for wild-type GFP and other proteins. GFP photoconversion was more efficient when using higher energy UV light (3.3–3.7 eV or 340–380 nm).[11] A more detailed study of Elowitz *et al.* reported that illumination of GFP by blue light converts GFP to a stable (under anaerobic conditions) form that absorbs green light at 2.36 eV (525 nm) and emits green, yellow, and red light (emission maxima at 2.21, 2.10, and 2.07 eV).[12] Based on the measured timescale of brightening (0.7 s), this study sug-

[a)]Electronic mail: epifanov@usc.edu.
[b)]Also at Institute of Biochemical Physics, Russian Academy of Sciences, Moscow 119334, Russia.
[c)]Electronic mail: krylov@usc.edu.

gested that the photoactivation proceeds in two steps: blue light (2.54 eV, 488 nm) stimulates a fast transition to an excited intermediate which then decays slowly to the red-emitting GFP state (the second step can proceed in the dark).

Recently, photoinduced redding of GFP has been observed under aerobic conditions.[13] In the presence of different oxidizing agents [e.g., $K_3Fe(CN)_6$, benzoquinone, etc.], irradiation with 2.54 eV (488 nm) light results in the bleaching of the green fluorescence and the appearance of the red signal with excitation and emission maxima at 2.16 eV (575 nm) and 2.04 eV (607 nm), respectively. Measurements at different light intensities determined that the redding is a one-photon process. Based on kinetic data, which showed that the green fluorescence disappears faster than the red fluorescence builds up, a two-step mechanism involving oxidation of GFP was suggested.[13] By testing a variety of electron acceptors, it was found that the redding was achieved using compounds with the standard reduction potential E° in the range of +0.42 to −0.32 V. The yield of the redox reaction between GFP and cytochrome c is 1.7 suggesting that a two-electron oxidation of GFP is responsible for the redding (that is, two reduced cytochrome c molecules are produced per one converted GFP molecule). The stability of the red form under the aerobic conditions points out that the mechanisms of anaerobic and oxidative redding are, most likely, different.[13] Moreover, the excitation spectra of the two forms are different: the maxima are at 2.36 and 2.16 eV (525 and 575 nm) for anaerobic and oxidative redding forms of GFP, respectively. Bogdanov *et al.*[13] hypothesized that anaerobic redding proceeds by photoreduction producing a stable radical (which will be sensitive to the presence of oxygen). Their findings suggest that oxidative redding produces more stable species. Other GFP variants, i.e., AcGFP1, TagGFP, zFP506, amFP486, and ppuGFP2 also undergo oxidative redding, however, the blue and cyan mutants (that have different chromophores) of GFP (EBFP and ECFP) do not.[13]

Theoretical modeling noticeably contributes to the studies of the GFP and related model systems[14–26] (for a recent review, see Ref. 27). In this paper we characterize the electronic structure of two different oxidized states of the deprotonated 4′-hydroxybenzylidene-2,3-dimethylimidazolinone (HBDI) anion (Fig. 1). We consider singly and doubly oxidized forms and discuss excitation energies and oscillator strengths of the electronic transitions in these species. To avoid confusion, it is important to clarify the terminology. Here we refer to deprotonated HBDI as the HBDI anion, or simply the anion. The (neutral) species derived by removing one electron from the anion is called the HBDI radical, and doubly oxidized deprotonated HBDI is called the HBDI cation. We also present the relevant ionization energies and estimate standard reduction potentials corresponding to these oxidation steps. The calculations are performed for the isolated gas-phase chromophores, however, possible effects of the solvent on reduction potentials are also discussed.

The protein environment is crucial for the function of the chromophore. The rigid protein matrix restricts the chromophore's range of motions and impedes the twisting motion in the excited state, which strongly affects the S_1-S_0 oscillator strength. For example, the chromophore in solution

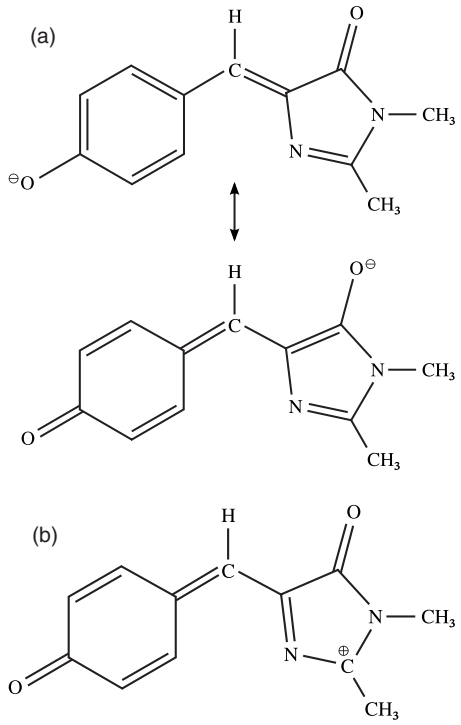

FIG. 1. Structures of deprotonated HBDI (HBDI anion, top) and the cation (bottom). The structure of the radical is similar to that of the cation, with the unpaired electron being on the carbon that hosts positive charge in the cation.

does not fluoresce, and the fluorescence is restored only in glass matrices.[4] The irreversible photoinduced conversion of the neutral to the anionic form also involves the protein. It is facilitated by a hydrogen bond network[28–30] and can be coupled to the decarboxylation of the glutamate 222 residue.[8,9] The electrostatic field of the protein may induce spectral shifts, although gas-phase studies suggested that the effect of the protein environment on the excited states energies may be relatively small.[31,32] Despite the role of the protein, an important step toward understanding the function of GFP is characterization of the intrinsic properties of the isolated chromophore. By focusing on the electronic properties of the chromophore, we can quantify changes in absorption and fluorescence due to specific structural changes and to test different mechanistic ideas. Our calculations show that the absorption of the singly oxidized species (radical) is blue-shifted with respect to the HBDI anion. However, the doubly oxidized system (cation), which has a stable closed-shell electronic structure, features redshifted absorption at 2.02 eV. The proposed mechanism involves two-step oxidation proceeding via electronically excited states.

II. COMPUTATIONAL DETAILS

Theoretical methods employed in this study are discussed in detail in our previous work.[22] Below we only briefly outline the essential details of the present calculations.

Equilibrium geometries of closed-shell ground-state species (i.e., the HBDI anion and the cation) were optimized by RI-MP2/cc-pVTZ. The structure of the anion is from Ref. 22. The ground state structure of the doublet radical was com-

puted using ωB97X/6-311(+,+)G(2df,2pd). The harmonic vibrational frequencies and IR intensities of the anionic and cationic forms of deprotonated HBDI were computed with RI-MP2/cc-pVTZ.

Excitation energies of the cation were computed using SOS-CIS(D) and EOM-EE-CCSD. SOS-CIS(D) calculations employed the cc-pVTZ and cc-pVDZ bases.[33] EOM-CCSD calculations used the 6-311G* basis set.[34,35] For the anion, SOS-CIS(D) excitation energies are in excellent agreement with MR-PT.[22] The oscillator strengths for SOS-CIS(D) were computed using the underlying CIS wave functions, whereas for EOM-EE-CCSD, the transition density matrices computed using EOM-EE wave functions were employed.

Electronic structure calculations for the open-shell radical species are more challenging due to spin contamination of the doublet reference. This effect can be mitigated by using better reference orbitals, e.g., those optimized for the MP2 wave function, i.e. the O2 method. We employed O2 orbitals in the SOS-CIS(D) calculations of the doublet states. Moreover, excited states in doublet radicals can develop a notable doubly excited character causing poor performance of single-reference methods using the doublet reference.[36–39] This can be avoided by employing the spin-flip (SF) methods[40–42] utilizing a high-spin quartet reference, i.e., $(\pi_2)^1(\pi_1)^1(\pi^*)^1$. The SF approach mitigates spin contamination and provides more balanced description of the ground and relevant excited states. Our EOM-SF-CCSD calculations (which employed B3LYP orbitals to control spin contamination of the quartet reference) showed that the wave functions of the excited states are of singly excited character (with respect to the doublet reference) thus validating the SOS-CIS(D) results. The $\langle S^2 \rangle$ values for the three lowest states of the doublet are 0.78. 0.79, and 0.81. The EOM-SF-CCSD and SOS-CIS(D) calculations are in quantitative agreement. Finally, MR-PT calculations of the doublet states are also in agreement with EOM-SF-CCSD and SOS-CIS(D).

MR-PT calculations employed a modified version of second-order multiconfigurational quasidegenerate perturbation theory (MCQDPT2).[43] Originally, the corresponding programs were implemented in GAMESS (U.S.)[44] and PC GAMESS.[45] Recently, serious bugs in the MCQDPT2 algorithm were noticed[46] and resolved in the new variant called XMCQDPT2 as implemented in PC GAMESS/FIREFLY.[46]

The XMCQDPT2 calculations used the complete active space self-consistent field (CASSCF) state-averaged (SA) electron density over several lowest-lying states. As CASSCF does not account for dynamical electron correlation,[47] the CASSCF state ordering is often different from the correct order predicted by higher-level calculations. This is the case for the doublet radical: the fourth lowest-lying state in the XMCQDPT2 calculation appears as the seventh in CASSCF. Since it is one of the states of interest (i.e., the D_2 state whose orbital character is described below), we had to use an extensive state-averaging procedure including eight states in the consideration. The active space for SA-CASSCF was chosen as 12 electrons distributed over 11 orbitals, which is a truncated representation of the complete set of 14 π-orbitals forming the conjugated system of the chromophore. The respective MOs and their populations are given in supplementary materials.[48] The MCQDPT2 based approaches have been shown to yield accurate results for a variety of chromophores.[43,49,50] The underlying CASSCF wave functions are free of spin contamination.

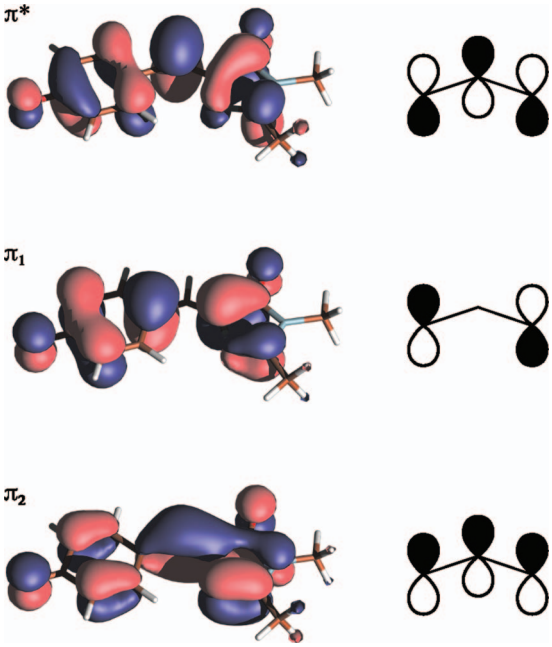

FIG. 2. Relevant molecular orbitals of deprotonated HBDI (HF/6-311G*). In the ground state of the anion, both π_1 and π_2 are doubly occupied, and the bright state is derived by the $\pi_1 \rightarrow \pi^*$ excitation. Oxidized forms are derived by removing the electrons from π_1.

The energy differences between different oxidized states were computed as follows. The vertical energy difference between the anion and the neutral radical, i.e., the first vertical detachment energy (VDE), was computed by EOM-IP-CCSD/6-311G* (2.33 eV) and corrected for basis set increase from 6-311G* to aug-cc-pVTZ using the Koopmans estimate (0.21 eV). Thus, our best estimate of VDE is 2.54 eV.

The vertical energy gap between the cation and the anion is computed as the difference between the RI-MP2/cc-pVTZ total energies of the respective species. The differences between the doublet and the cation were computed from the relative energies of the cation and the anion and the anion's VDE. Finally, the adiabatic values were obtained from vertical gaps by using relaxation energies of the neutral and the cation, which were computed by RI-MP2/cc-pVTZ (cation) and ωB97X/6-311(+,+)G(2df,2pd) (radical) using the geometries described above.

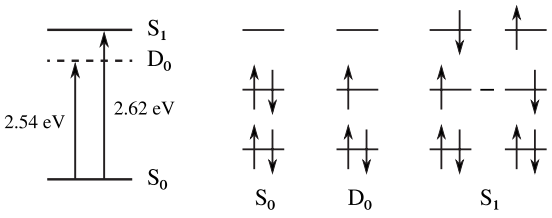

FIG. 3. Energy levels and electronic states of the HBDI anion and radical. The bright absorbing $\pi_1\pi^*$ state at 2.62 eV is a resonance state embedded in a photodetachment continuum beginning at 2.54 eV. The respective MOs are shown in Fig. 2.

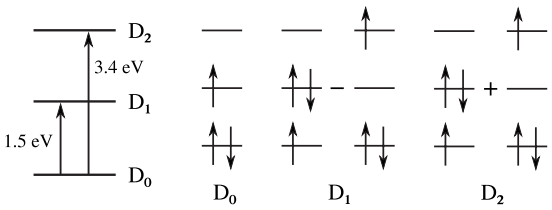

FIG. 4. Electronic states of the doublet HBDI radical. The respective MOs are shown in Fig. 2.

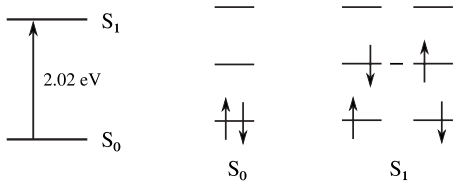

FIG. 5. Electronic states of the doubly ionized HBDI anion. The respective MOs are shown in Fig. 2.

EOM and SOS-CIS(D) calculations were performed using Q-CHEM.[51] XMCQDPT2 calculations were carried out with PC GAMESS/FIREFLY.[45] All relevant structures and energies as well as MOs are available in supporting materials.[48]

III. RESULTS AND DISCUSSION

Relevant MOs and electronic states of the gas-phase HBDI anion are shown in Figs. 2 and 3. Gas-phase photodestruction spectra show the absorption maximum of the anionic GFP chromophore at 2.59 eV,[31,32] which is remarkably close to the absorption of wild-type GFP at 2.61 eV. Most of the electronic structure studies agree on the character of the bright state,[14–17,19,21,22,24,25,52] which is of a $\pi \rightarrow \pi^*$ type (Fig. 2), although there is a spread in reported excitation energies. Our recent theoretical study revealed that the bright state is, in fact, a resonance state embedded in a photodetachment continuum.[22] These calculations determined that the VDE of the HBDI anion is 2.4–2.5 eV, which is below the bright state. A recent experimental study,[53] which also employed electronic action spectroscopy, reported the vertical excitation energy of 2.60 eV and determined VDE to lie within 2.48–2.8 eV, in excellent agreement with our prediction.

As evident from Fig. 3, the electronic excitation using 2.6 eV (and higher) produces the excited state that can photodetach an electron producing a doublet neutral radical. Thus, our first step is to characterize electronic transitions of this form. Three lowest electronic states of the doublet and the corresponding excitation energies and oscillator strengths are shown in Fig. 4 and summarized in Table I. The MOs of the radical are very similar to those of the anion and are given in supplementary materials.[48] The ground state of the doublet is derived by the ionization from the anion's highest occupied molecular orbital (HOMO) (π_1 from Fig. 2). The two excited states are of a mixed character and include almost equal contributions from the $\pi_1 \rightarrow \pi^*$ and $\pi_2 \rightarrow \pi^*$ excitations. Consistently with the allylic character of the three relevant MOs, both excitations have large transition dipole moments, and their plus and minus combinations give rise to the bright and dark states (see Appendix) at 4.14 eV (f_l =1.04) and 1.93 eV (f_l=0). The SOS-CIS(D) and MR-PT calculations agree with EOM-SF-CCSD on the character of the excited states and yield slightly lower excitation energies. Overall, the bright state of the doublet is strongly blueshifted relative to the anionic form. Therefore, the doublet radical is an unlikely candidate for the red GFP form. The energy spacing between the two excited doublet states is 2.21 eV and the oscillator strength is non-negligible (0.01). Thus, redshifted electronic transitions between D_2 and D_1 are possible.

TABLE I. Vertical excitation energies (eV) and oscillator strengths of the $\pi\pi^*$ states of the doublet HBDI radical. The values of $\langle S^2 \rangle$ are also shown.

Method	D_1	$\langle S^2 \rangle$	D_2	$\langle S^2 \rangle$
SOS-CIS(D)/cc-pVDZ[a]	1.64(0.02)	1.04	3.53(1.35)	0.90
SOS-CIS(D)/cc-pVTZ[a]	1.52(0.02)	1.01	3.37(1.34)	0.89
EOM-SF-CCSD/6-311G* [b]	1.93(0.01)	0.79	4.14(1.04)	0.81
XMCQDTP2/6-311G* [c]	1.80(0.01)		3.27(0.66)	

[a]Using O2 orbitals. Oscillator strength are computed at the CIS level.
[b]Using B3LYP orbitals.
[c]Based on SA(8)-CASSCF(12/11).

Doubly ionized HBDI anion (i.e., the cation) is a closed-shell system derived by removing two electrons from π_1. Its electronic states are summarized in Fig. 5 and in Table II. The respective MOs are similar to those of the anion and are given in supplementary materials.[48] The lowest singlet excited state ($^1A'$) is at 2.02 eV [SOS-CIS(D)/cc-pVTZ] and has a large oscillator strength. It is redshifted relative to the $S_0 \rightarrow S_1$ transition in the anion by 0.6 eV, which is similar in magnitude to the observed experimental shift in absorption. The EOM-EE-CCSD excitation energy is higher, but the shift relative to the EOM-EE value of the S_1 excitation energy in the anion (at 3.1 eV at the EOM-EE/6-311G* level) is very close to the SOS-CIS(D) one. Thus, this species is a possible candidate for the red fluorescent form of GFP produced in oxidative redding experiments.[13]

The redshift is consistent with the changes in the character of the electronic transition, which is a $\pi_2 \rightarrow \pi_1$ excitation, as opposed to the $\pi_1 \rightarrow \pi^*$ transition in the anion. Thus, in terms of the anionic orbitals, the S_1 state of the cation is HOMO-1 $\rightarrow$ HOMO excitation. Because of a relatively dense spectrum of the occupied orbitals (which becomes even denser in the positively charged system), the gap between HOMO-1 and HOMO is smaller than the gap between the HOMO and the lowest unoccupied molecular orbital. Thus, double ionization is expected to result in a red shift in the lowest electronic transition.

Interestingly, the $\pi_2 \rightarrow \pi^*$ state of the cation is much higher in energy (approximately at 3.16 eV, f_l=0.0261). The

TABLE II. Vertical excitation energies (eV) and oscillator strengths of the excited states of the HBDI cation at its equilibrium geometry.

Method	$^1A'(f_l)$	$^1A''$
SOS-CIS(D)/cc-pVDZ[a]	2.10(1.20)	2.14
SOS-CIS(D)/cc-pVTZ[a]	2.02(1.17)	2.09
EOM-CCSD/6-311G*	2.53(0.78)	2.10
XMCQDTP2/6-311G* [b]	2.27(0.84)	

[a]Oscillator strength are computed at the CIS level.
[b]Based on SA(2)-CASSCF(12/11).

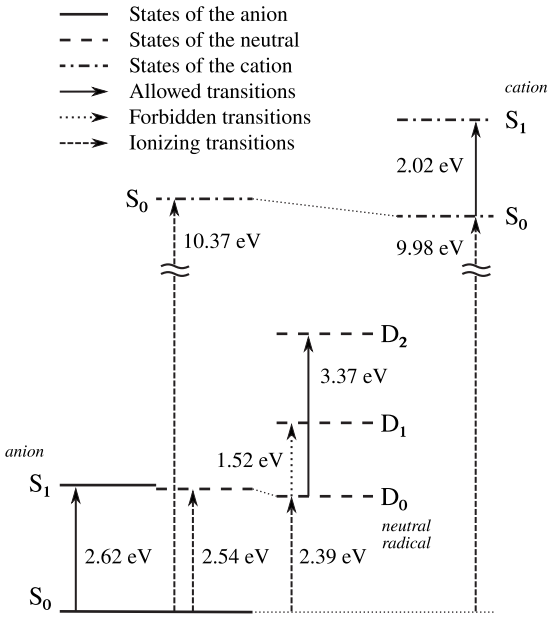

FIG. 6. Energy diagram of the relevant electronic states of deprotonated HBDI.

closest electronic state is a dark state, $^1A''$ derived from the HOMO-3→HOMO transition (in terms of the anionic orbitals).

Figure 6 shows an overall energy diagram for the three forms of HBDI. Adiabatically, the doubly oxidized form is 9.98 eV above the ground state of the anion. The respective value of VDE (corresponding to removing two electrons) is 10.37 eV. The adiabatic IE from the ground state of the doublet radical is 7.59 eV (computed using the anion's VDE value of 2.54 and 0.15 eV relaxation energy of the neutral radical). Another relevant value is the energy gap between the excited states (D_1 and D_2) of the doublet radical and the cation. Using the same values of vertical detachment and relaxation energies, and 1.52 and 3.37 eV for the vertical $D_0 \rightarrow D_{1,2}$ excitation energies, we estimate the ionization energy of the electronically excited doublet radical as 6.07 and 4.22 eV, respectively. Finally, the energy gap between the excited singlet state of the anion and the two excited states of the radical are 1.29 and 3.14 eV, respectively.

To evaluate whether two-electron oxidation of the anion is possible using the electron acceptors employed in Ref. 13, it is necessary to estimate standard reduction potentials corresponding to the detachment and ionization transitions described above. Rigorous calculations of the oxidation/reduction potentials require free energy calculations, however, a simpler approach based on the correlation between detachment/ionization energies and the standard reduction potentials can be employed:[54]

$$E^\circ = (-2.59 \pm 0.26) + (0.56 \pm 0.03) \cdot \mathrm{VIE}, \quad (1)$$

where E° corresponds to the following half reaction:

$$A^+ + e = A, \quad (2)$$

and VIE is the ionization energy of A. This equation was derived by comparing experimental values of the reversible oxidation potentials (in DMF or ACN solvent) for a set of 14 organic molecules with their gas-phase ionization energies. Applying this equation, we arrive at the values of E° summarized in Table III. Equation (1) was derived using IEs in the range of 5.6–9.0 eV and its application to lower values (such as the $S_1 \rightarrow D_{1,2}$ transitions from Table III) assumes that the trend can be extrapolated. Thus, estimations for the lower IEs are of a semiquantitative value only.

TABLE III. Standard oxidation potentials corresponding to different one-electron oxidation transitions computed using gas-phase detachment and ionization energies (see text).

Transition	IE (eV)	E° (V)
$D_0 \rightarrow$ cation	7.59	1.66 ± 0.49
$D_1 \rightarrow$ cation	6.07	0.81 ± 0.44
$D_2 \rightarrow$ cation	4.22	-0.23 ± 0.39
$S_1 \rightarrow D_1$	1.29	-1.87 ± 0.30
$S_1 \rightarrow D_2$	3.14	-0.83 ± 0.35

Oxidation of the ground-state doublet radical (D_0) corresponds to $E^\circ = 1.66$ V, which is much larger than E° of the strongest oxidizing agent employed in Ref. 13 ($K_3Fe(CN)_6$, $E^\circ = 0.42$ V). However, the oxidation of the electronically excited neutral radical corresponds to $E^\circ = 0.81$ V and $E^\circ = -0.12$ V for the D_1 and D_2 states, respectively. Thus, electronically excited doublet radical (in the D_2 state) can be oxidized even by the weakest oxidizing agent from Ref. 13 ($E^\circ = -0.32$ V), whereas the oxidation of D_1 is less likely. Finally, the electronically excited anion can be easily oxidized producing excited states of the doublet ($E^\circ = -1.87$ V and $E^\circ = -0.83$ V for D_1 and D_2 states, respectively). Note that the $S_1 \rightarrow D_0$ transition is spontaneous in the gas phase and does not require the presence of oxidizing agents due to the autoionizing nature of S_1. By comparing the electronic configurations of the doublet states (see Fig. 4) and the S_1 state (Fig. 3), we note that these transitions include significant one-electron character. Thus, a possible mechanism of the oxidative redding emerging from the present study is presented in Scheme 1.

The first step involves photoexcitation, and the blue light is sufficient to generate this transition. The second and third steps are one-electron oxidation steps with $E^\circ = -0.88$ V, which is within the reach of the oxidizing agents employed in Ref. 13. The two-electron oxidation is consistent with the stoichiometric results from Ref. 13. Moreover, the closed-shell character of the cation is consistent with the relatively chemically stable nature of the red form of GFP. Although the chemical structure of the cation suggests high reactivity with respect to nucleophilic agents (e.g., water), the protein may be sufficiently effective in shielding this fragile species. Finally, the absorption of the cationic form is redshifted by

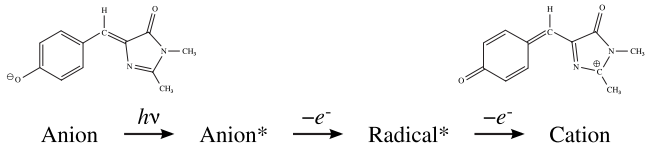

SCHEME 1. Possible mechanism of one-photon two-electron oxidation of the deprotonated HBDI anion.

TABLE IV. Selected geometric parameters (bond lengths in angstrom, angles in degrees) of the deprotonated HBDI anion, and its singly and doubly oxidized forms.

Species	C_P-C_B	C_I-C_B	$C_P-C_B-C_I$	O_P-C	O_I-C
Anion[a]	1.393	1.385	134.8	1.248	1.236
Cation[a]	1.386	1.389	127.8	1.226	1.197
Radical[b]	1.413	1.369	129.6	1.228	1.209

[a]RI-MP2/cc-pVTZ.
[b]ωB97X/6-311(+,+)G(2df,2pd).

0.6 eV, and the resulting value of 2.02 eV is in a good agreement with the experimental excitation energy of 2.12 eV. Finally, structural differences between the chromophores of the FPs that undergo oxidative redding (AcGFP1, TagGFP, zFP506, amFP486, and ppuGFP2), and those that do not (EBFP and ECFP) provide additional support to the proposed mechanism. The chromophores in the former group contain a phenolic moiety that can be easily converted to the anionic deprotonated form and thus oxidized, whereas in EBFP and ECFP the imidazolin moiety is connected to nitrogen-containing aromatic fragments that are expected to be basic rather than acidic.

Whereas the present model is consistent with the available experimental information, it cannot rule out possible involvement of the protein via proton transfer or other chemical changes (such as covalent bond breaking leading to the extension of the π-system of the chromophore).[7,26] Thus, it would be desirable to observe oxidative redding in the isolated chromophore, e.g., in solution. However, it is essential for the proposed mechanism that the excited states involved in oxidation, S_1 of the anion and $D_{1,2}$ of the radical, are relatively long lived. Thus, it may be problematic to observe oxidative redding of isolated HBDI in solution, where the internal conversion is markedly faster than in the protein (which is responsible for the loss of fluorescence), except for low-temperature glass matrices (in which fluorescence is restored). Finally, the protein environment may change the predicted energetics by stabilizing different states differently. However, the observed strong redshift in the doubly oxidized species originates in strong changes in the electronic structure of the chromophore, and it is unlikely that the energies of these transitions will be affected by the protein much stronger than the energies of the transitions in the anion. Our preliminary QM/MM calculations, which treated the chromophore and the nearest amino acid side chains as the quantum subsystem and the rest of the model protein system as the collection of effective fragments, do not show dramatic structural changes in the chromophore binding site for the anionic and cationic species. We also note that the present model does not address the nature of the anaerobic redding of GFP, which will be discussed elsewhere.

A. Ionization-induced structural changes

As discussed in Ref. 22, the equilibrium structure the HBDI anion can be explained by considering two resonance structures shown in Fig. 1 (upper panel). Consequently, the negative charge is delocalized between the phenolic and imidazolin oxygens and the C_I-C_B and C_P-C_B bond orders are scrambled.[22] The analysis of the structural parameters and the wave functions demonstrated that the phenolic form dominates, i.e., the C_P-C_B bond is longer than C_I-C_B. Double ionization eliminates the phenolic structure entirely producing the quinoid structure shown in Fig. 1 (bottom). The positive charge located on the imidazolin carbon is stabilized by electron-donating methyl group (the NBO analysis[55] suggests considerable delocalization of the hole over imidazolin moiety). The structure of the radical can be described as the quinoid structure with the unpaired electron on the imidazolin's methyl-substituted carbon.

Table IV summarizes important geometric parameters of the anion, neutral, and the cation (full geometries are given in supplementary materials).[48] Consistently with the above analysis, both CO bonds become shorter in the cation, and the C_P-C_B bond becomes shorter than C_I-C_B. However, the bond alternation remains small due to conjugation. Moreover, because of the two resonance structures present in the anion, the overall structural differences between the anion and the cation are less than could be expected by considering only the dominant phenolate structure.

The ionization-induced structural changes strongly affect vibrational frequencies, which may be exploited in the experimental characterization of the red form of GFP, e.g., by using IR or Raman spectroscopy as in Refs. 56 and 9 (a detailed summary of the vibrational spectroscopy studies of GFP can be found in Ref. 57). Figure 7 shows the computed IR spectra of anionic and cationic deprotonated HBDI (a full list of harmonic frequencies is given in supplementary materials).[48] The anion spectrum is dominated by a band at 1691 cm^{-1}, which is an asymmetric CO stretch strongly coupled with an asymmetric bridge vibration. In the cation, this mode changes its character to an almost pure bridge

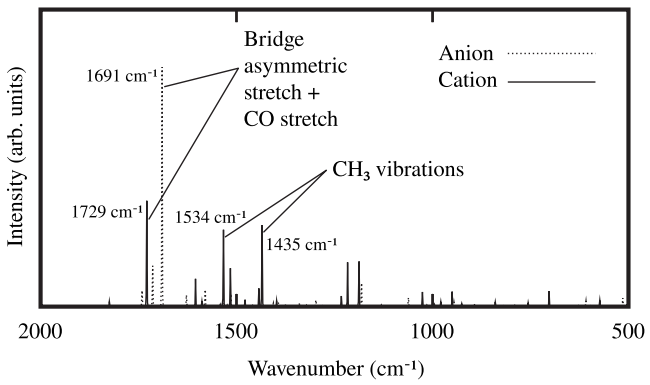

FIG. 7. Infrared spectra of the anionic and cationic forms of deprotonated HBDI computed with RI-MP2/cc-pVTZ.

vibration, loses intensity and is blueshifted. Instead, the modes that involve the positively-charged imidazolin moiety gain intensity. The two most intense bands are predominantly CH_3 vibrations at 1534 and 1435 cm^{-1}, followed by lower frequency bands involving skeletal imidazolin vibrations.

IV. CONCLUSIONS

We characterized changes in the electronic structure of the deprotonated HBDI anion due to one- and two-electron oxidation processes. One-electron oxidation produces a doublet radical with strongly blueshifted absorption, whereas the absorption in the cation is redshifted by almost 0.6 eV with respect to the anion. From the electronic structure point of view, the cation has a closed-shell singlet ground state, and is expected to be relatively stable chemically, especially in the protective and hydrophobic protein environment.

Our results suggest that the doubly oxidized species (the deprotonated HBDI cation) may be responsible for the oxidative redding of GFP, which was recently reported.[13] The proposed mechanism involves two-step oxidation via electronically excited states and is consistent with the available experimental information,[13] i.e., it is a one-photon process including two-electron oxidation resulting in chemically stable species. Moreover, all proteins that undergo oxidative redding contain a phenolic moiety and are expected to have similar oxidative properties, whereas the two proteins that do not exhibit redding (EBFP and ECFP) have nitrogen-containing aromatic fragments that are less efficient electron donors. This suggests that the oxidative redding is an intrinsic property of the chromophore, although chemical changes involving the protein cannot be ruled out. Moreover, the irreversible nature of the oxidative redding[13] suggests that the protein is likely to change in response to the changes in the chromophore's oxidation state. Ionization-induced structural changes of the chromophore result in significant changes in vibrational spectra (the frequencies as well as the character of the modes and IR intensities) which may be exploited in the experimental validation of the proposed mechanism.

We would like to emphasize that simple molecular orbital considerations predict redshifted absorption for any doubly oxidized species. Thus, while the predicted values of the absorption maximum may change once the protein environment is taken into account (or at a higher level of theory), the overall trend remains unchanged. This mechanism of redding is distinctly different from previously characterized ones in which redding was achieved by extending the π-system of the chromophore.[7]

ACKNOWLEDGMENTS

This work was conducted under the auspices of the iOpenShell Center for Computational Studies of Electronic Structure and Spectroscopy of Open-Shell and Electronically Excited Species (http://iopenshell.usc.edu) supported by the National Science Foundation through the Grant No. CRIF:CRF CHE-0625419+0624602+0625237, as well as through Grant No. CHE-0616271 grant (A.I.K.). We thank Dr. Ksenia Bravaya for generous help and valuable discussions of this work. This work is supported by the joint grant from the U.S. Civilian Research and Development Foundation (Project No. RUC1-2914-MO-07) and the Russian Foundation for Basic Research (Grant No. 08-03-91104-AFGIR). I.P., B.G., and A.N. thank the SKIF-GRID program for providing resources at the SKIF-MSU, SKIF-SIBERIA, and UGATU computational facilities.

APPENDIX: CHARACTER OF THE ELECTRONIC STATES OF THE NEUTRAL RADICAL AND THE CATION

As shown in Fig. 2, the frontier MOs of HBDI are of allylic character in the bridge region. This isomorphism has been discussed and exploited.[18,58] The allyliclike orbital character explains the bond alternation pattern and is responsible for a reduced barrier for the *cis-trans* isomerization in the ground electronic state.[22,23] Earlier applications of the Hückel-like and simpler models to dyes explained changes in the absorption wavelengths upon substitutions[59] and excited state charge separation coupled with *cis-trans* isomerization.[60]

Below we use a simple Hückel picture to explain oscillator strengths of the two lowest electronic transitions of the doublet radical and the cation. The Hückel description of the three MOs from Fig. 2 in the bridge region is

$$\pi_2 = \frac{1}{\sqrt{3}}(p_A + p_B + p_C), \tag{A1}$$

$$\pi_1 = \frac{1}{\sqrt{2}}(p_A - p_C), \tag{A2}$$

$$\pi^* = \frac{1}{\sqrt{3}}(p_A - p_B + p_C), \tag{A3}$$

where p_A, p_B, and p_C are p-orbitals of the three bridge carbon atoms, C_{1P}, C_{1B}, and C_{1I}, respectively. For the sake of simplicity, consider linear arrangement of the atoms such that p_B is located at $x=0$, and p_A and p_C—at $\mp x_0$, such that $\langle p_B|x|p_B\rangle = 0$ and $\langle p_{A,C}|x|p_{A,C}\rangle = \mp x_0$. The transition dipole moments matrix elements are

$$\langle \pi_1|x|\pi^*\rangle = \frac{1}{\sqrt{6}}\langle p_A - p_C|x|p_A - p_B + p_C\rangle \approx \frac{1}{\sqrt{6}}(\langle p_A|x|p_A\rangle - \langle p_C|x|p_C\rangle) = -\frac{2}{\sqrt{6}}x_0, \tag{A4}$$

$$\langle \pi_2|x|\pi^*\rangle = \frac{1}{\sqrt{9}}\langle p_A + p_B + p_C|x|p_A - p_B + p_C\rangle \approx \frac{1}{3}(\langle p_A|x|p_A\rangle - \langle p_B|x|p_B\rangle + \langle p_C|x|p_C\rangle) = 0, \tag{A5}$$

$$\langle \pi_2|x|\pi_1\rangle = \frac{1}{\sqrt{6}}\langle p_A + p_B + p_C|x|p_A - p_C\rangle$$

$$\approx \frac{1}{\sqrt{6}}(\langle p_A|x|p_A\rangle - \langle p_C|x|p_C\rangle) = -\frac{2}{\sqrt{6}}x_0, \quad \text{(A6)}$$

where we again assumed zero overlap between the orbitals centered on different atoms.

The S_1 state of the anion is derived from the $\pi_1 \rightarrow \pi^*$ transition, and the value of the transition matrix element $|\langle \pi_1|x|\pi^*\rangle|^2 = (2/3)x_0^2$ explains its large oscillator strength. In the cation, two electronic transitions are possible, $\pi_2 \rightarrow \pi^*$ and $\pi_2 \rightarrow \pi_1$, however, the former is expected to have zero oscillator strength (and is also considerably higher in energy), whereas the latter should be as bright as the $\pi_2 \rightarrow \pi^*$ transition in the anion. Note that the character of the target orbital is different in the S_1 states of the anion and the cation.

In the doublet radical, the excited states are derived from the out-of-phase and in-phase combinations of the $\pi_2 \rightarrow \pi^*$ and $\pi_2 \rightarrow \pi_1$ transitions. Because the respective dipole moment matrix elements have the same magnitude, one of the states is dark, whereas the second is bright, which explains the computed values of the oscillator strengths for D_1 and D_2.

The above Hückel treatment predicts that all three bright transitions have the same $\langle \mu_{tr} \rangle$. The computed values (CIS/cc-pVTZ) of $|\langle \mu_{tr} \rangle|^2$ are indeed very close and equal 16.43, 13.99, and 14.04 a.u. for the anion, radical, and the cation transitions, respectively. The corresponding values of x_0 are 2.6, 1.6, and 2.4 Å are larger than the CC bondlength (1.4 Å) indicating a degree to which the extended MOs from Fig. 2 differ from their simple allylic representation.

Note that this simple Hückel model predicts the same excitation energies for the $\pi_1 \rightarrow \pi^*$ and the $\pi_2 \rightarrow \pi_1$ transitions, and one needs to take into account differences in the orbital energies (i.e., already at the Hartree–Fock level, one would expect that the $\pi_2 - \pi_1$ gap is smaller than $\pi_1 - \pi^*$) and their changes upon ionization (denser orbital spectrum in the cation due to increased Coulomb attraction to the positively charged core) to explain the redshift in the excitation energies.

[1] R. Y. Tsien, Annu. Rev. Biochem. **67**, 509 (1998).
[2] M. Zimmer, Chem. Rev. (Washington, D.C.) **102**, 759 (2002).
[3] Y. Wang, J. Y.-J. Shyy, and S. Chien, Annu. Rev. Biomed. Eng. **10**, 1 (2008).
[4] S. R. Meech, Chem. Soc. Rev. **38**, 2922 (2009).
[5] V. Sample, R. H. Newman, and J. Zhang, Chem. Soc. Rev. **38**, 2852 (2009).
[6] N. C. Shaner, G. H. Patterson, and M. W. Davidson, J. Cell Sci. **120**, 4247 (2007).
[7] K. A. Lukyanov, D. M. Chudakov, S. Lukyanov, and V. V. Verkhusha, Natl. Prod. Rev. **6**, 885 (2005).
[8] J. J. van Thor, T. Gensch, K. J. Hellingwerf, and L. N. Johnson, Nat. Struct. Biol. **9**, 37 (2002).
[9] A. F. Bell, D. Stoner-Ma, R. M. Wachter, and P. J. Tonge, J. Am. Chem. Soc. **125**, 6919 (2003).
[10] M. Andresen, A. S. Stiel, S. Trowitzsch, G. Weber, C. Eggeling, M. Wahl, S. W. Hell, and S. Jackobs, Proc. Natl. Acad. Sci. U.S.A. **104**, 13005 (2007).
[11] K. E. Sawin and P. Nurse, Curr. Biol. **7**, R606 (1997).
[12] M. B. Elowitz, M. G. Surette, P. E. Wolf, J. Stock, and S. Liebler, Curr. Biol. **7**, 809 (1997).
[13] A. M. Bogdanov, A. S. Mishin, I. V. Yampolsky, V. V. Belousov, D. M. Chudakov, F. V. Subach, V. V. Verkhusha, S. Lukyanov, and K. A. Lukyanov, Nat. Chem. Biol. **5**, 459 (2009).
[14] A. A. Voityuk, M.-E. Michel-Beyerle, and N. Rösch, Chem. Phys. Lett. **272**, 162 (1997).
[15] W. Weber, V. Helms, J. A. McCammon, and P. W. Langhoff, Proc. Natl. Acad. Sci. U.S.A. **96**, 6177 (1999).
[16] V. Helms, C. Winstead, and P. W. Langhoff, J. Mol. Struct.: THEOCHEM **506**, 179 (2000).
[17] M. E. Martin, F. Negri, and M. Olivucci, J. Am. Chem. Soc. **126**, 5452 (2004).
[18] S. Olsen and S. C. Smith, J. Am. Chem. Soc. **130**, 8677 (2008).
[19] I. A. Topol, J. Collins, I. Polyakov, B. L. Grigorenko, and A. V. Nemukhin, Biophys. Chem. **145**, 1 (2009).
[20] B. G. Levine and T. J. Martinez, Annu. Rev. Phys. Chem. **58**, 613 (2007).
[21] K. B. Bravaya, A. V. Bochenkova, A. A. Granovsky, and A. V. Nemukhin, Khim. Fiz. **27**, 13 (2008) (in Russian).
[22] E. Epifanovsky, I. Polyakov, B. L. Grigorenko, A. V. Nemukhin, and A. I. Krylov, J. Chem. Theory Comput. **5**, 1895 (2009).
[23] I. Polyakov, E. Epifanovsky, B. L. Grigorenko, A. I. Krylov, and A. V. Nemukhin, J. Chem. Theory Comput. **5**, 1907 (2009).
[24] C. Filippi, M. Zicchedu, and F. Buda, J. Chem. Theory Comput. **5**, 2074 (2009).
[25] Y. Ma, M. Rohlfing, and C. Molteni, J. Chem. Theory Comput. **6**, 257 (2010).
[26] E. Sanchez-Garcia, M. Doerr, Y.-W. Hsiao, and W. Thiel, J. Phys. Chem. B **113**, 16622 (2009).
[27] A. V. Nemukhin, B. L. Grigorenko, and A. P. Savitskii, Acta Naturae **2**, 41 (2009).
[28] X. Shu, K. Kallio, X. Shi, P. Abbyad, P. Kanchanawong, W. Childs, S. G. Boxer, and S. J. Remington, Biochemistry **46**, 12005 (2007).
[29] X. Shi, P. Abbyad, X. Shu, K. Kallio, P. Kanchanawong, W. Childs, S. J. Remington, and S. G. Boxer, Biochemistry **46**, 12014 (2007).
[30] P. Leiderman, L. Genosar, D. Huppert, X. Shu, S. J. Remington, K. Solntsev, and L. M. Tolbert, Biochemistry **46**, 12026 (2007).
[31] S. B. Nielsen, A. Lapierre, J. U. Andersen, U. V. Pedersen, S. Tomita, and L. H. Andersen, Phys. Rev. Lett. **87**, 228102 (2001).
[32] L. H. Andersen, A. Lappierre, S. B. Nielsen, I. B. Nielsen, S. U. Pedersen, U. V. Pedersen, and S. Tomita, Eur. Phys. J. D **20**, 597 (2002).
[33] T. H. Dunning, J. Chem. Phys. **90**, 1007 (1989).
[34] W. J. Hehre, R. Ditchfield, and J. A. Pople, J. Chem. Phys. **56**, 2257 (1972).
[35] R. Krishnan, J. S. Binkley, R. Seeger, and J. A. Pople, J. Chem. Phys. **72**, 650 (1980).
[36] D. Maurice and M. Head-Gordon, Int. J. Quant. Chem. Symp. **56**, 361 (1995).
[37] D. Maurice and M. Head-Gordon, J. Phys. Chem. **100**, 6131 (1996).
[38] P. G. Szalay and J. Gauss, J. Chem. Phys. **112**, 4027 (2000).
[39] C. E. Smith, R. A. King, and T. D. Crawford, J. Chem. Phys. **122**, 054110 (2005).
[40] A. I. Krylov, Chem. Phys. Lett. **338**, 375 (2001).
[41] A. I. Krylov, Acc. Chem. Res. **39**, 83 (2006).
[42] A. I. Krylov, Annu. Rev. Phys. Chem. **59**, 433 (2008).
[43] H. Nakano, J. Chem. Phys. **99**, 7983 (1993).
[44] M. W. Schmidt, K. K. Baldridge, S. T. Elbert, J. A. Boatz, M. S. Gordon, S. Koseki, J. H. Jensen, N. Mastunaga, K. A. Nguyen, T. L. Windus, S. Su, M. Dupuis, and J. A. Montgomery, J. Comput. Chem. **14**, 1347 (1993).
[45] A. A. Granovsky, PC GAMESS/FIREFLY, http://classic.chem.msu.su/gran/gamess/index.html (accessed Dec. 18, 2009).
[46] A. A. Granovsky, XMCQDPT2, http://classic.chem.msu.su (accessed Dec. 18, 2009).
[47] T. Helgaker, P. Jørgensen, and J. Olsen, *Molecular Electronic Structure Theory* (Wiley, New York, 2000).
[48] See supplementary material at http://dx.doi.org/10.1063/1.3336425 for molecular orbitals, structures, and relative energies.
[49] K. Bravaya, A. Bochenkova, A. Granovsky, and A. Nemukhin, J. Am. Chem. Soc. **129**, 13035 (2007).
[50] L. H. Andersen and A. V. Bochenkova, Eur. Phys. J. D **51**, 5 (2009).
[51] Y. Shao, L. F. Molnar, Y. Jung, J. Kussmann, C. Ochsenfeld, S. Brown, A. T. B. Gilbert, L. V. Slipchenko, S. V. Levchenko, D. P. O'Neil, R. A. Distasio, Jr., R. C. Lochan, T. Wang, G. J. O. Beran, N. A. Besley, J. M. Herbert, C. Y. Lin, T. Van Voorhis, S. H. Chien, A. Sodt, R. P. Steele, V.

A. Rassolov, P. Maslen, P. P. Korambath, R. D. Adamson, B. Austin, J. Baker, E. F. C. Bird, H. Daschel, R. J. Doerksen, A. Drew, B. D. Dunietz, A. D. Dutoi, T. R. Furlani, S. R. Gwaltney, A. Heyden, S. Hirata, C.-P. Hsu, G. S. Kedziora, R. Z. Khalliulin, P. Klunziger, A. M. Lee, W. Z. Liang, I. Lotan, N. Nair, B. Peters, E. I. Proynov, P. A. Pieniazek, Y. M. Rhee, J. Ritchie, E. Rosta, C. D. Sherrill, A. C. Simmonett, J. E. Subotnik, H. L. Woodcock III, W. Zhang, A. T. Bell, A. K. Chakraborty, D. M. Chipman, F. J. Keil, A. Warshel, W. J. Herhe, H. F. Schaefer III, J. Kong, A. I. Krylov, P. M. W. Gill, and M. Head-Gordon, Phys. Chem. Chem. Phys. **8**, 3172 (2006).

[52] A. K. Das, J.-Y. Hasegawa, T. Miyahara, M. Ehara, and H. Nakatsuji, J. Comput. Chem. **24**, 1421 (2003).

[53] M. W. Forbes and R. A. Jockusch, J. Am. Chem. Soc. **131**, 17038 (2009).

[54] C. Crespo-Hernández, D. M. Close, L. Gorb, and J. Leszczynski, J. Phys. Chem. B **111**, 5386 (2007).

[55] E. D. Glendening, J. K. Badenhoop, A. E. Reed, J. E. Carpenter, and F. Weinhold, *NBO 4.0* (University of Wisconsin, Madison, 1996).

[56] J. J. van Thor, A. J. Pierik, I. Nugteren-Roodzant, A. Xie, and K. J. Hellingwerf, Biochemistry **37**, 16915 (1998).

[57] J. J. van Thor, Chem. Soc. Rev. **38**, 2935 (2009).

[58] S. Olsen and R. H. McKenzie, J. Chem. Phys. **130**, 184302 (2009).

[59] M. J. S. Dewar, J. Chem. Soc. 2329 (1950).

[60] M. Dekhtyar, W. Retting, and V. Rozenbaum, Photochem. Photobiol. **120**, 75 (1999).